

Fröhlich Condensate of Phonons in Optomechanical Systems

Xu Zheng^{1,*} and Baowen Li^{2,1,†}

¹*Department of Physics, University of Colorado, Boulder, CO, 80309, USA*

²*Paul M. Rady Department of Mechanical Engineering,
University of Colorado, Boulder, CO, 80309, USA*

(Dated: February 28, 2025)

We report the Fröhlich condensate of phonons in optomechanical systems. The system consists of a one-dimensional array of membranes coupled to the cavity field via a quadratic interaction, and the cavity is pumped by an external laser. Analytical and numerical results demonstrate that the high phonon occupancy of the lowest or highest mechanical mode is achievable depending on the detuning of the driving laser, the optomechanical strength, and the temperature. The decoherence of the Fröhlich condensate can be largely suppressed by the large number of membranes. Our results shed light on narrow-linewidth phonon laser, energy conversion/transfer, and efficient multimode cooling. Feasibility of experimental implementation is also discussed.

Introduction.— The study of open systems far from thermodynamic equilibrium has attracted attentions during the past decades. An interesting phenomenon in these systems is the emergence of collective behaviors and self-organization, which is the mechanism behind the generation of laser, superfluorescence [1], synchronization [2–6], etc. In biological systems, many theoretical works have suggested that the collective behavior may have profound effects on the chemical and enzyme kinetics [7], and the cognitive function of brain [8]. Among these works a widely used model is the Fröhlich condensate [9–11]. In 1968, Fröhlich showed that the energy of a collection of oscillators would concentrate at the lowest mode once the external energy supply exceeds a threshold. While this phenomenon is usually compared to the Bose-Einstein condensation [12, 13], the Fröhlich condensate is a nonequilibrium phenomenon. Many researchers have investigated the corresponding quantum Hamiltonian [14–16], the classification, the coherence and the phonon statistics [7, 17] of the Fröhlich condensate. Recently, the study has been extended to magnons [18, 19].

Despite intense investigations, no unambiguous identification of a Fröhlich condensate has been proved.

Misochko et.al. reported a Fröhlich condensate in a single crystal of bismuth but it is transient [20]. Reimers et.al showed that coherent Fröhlich condensate involves extremely large energies that are inaccessible in a biological environment [7]. Altfeder et.al reported the optical phonon condensate in heterostructures at room temperature, but their system is at thermal equilibrium [21]. Nardecchia et.al. reported a remarkable absorption feature around 0.314 THz in bovine serum albumin (BSA) when driven out of equilibrium by optical pumping, which might be a signal of Fröhlich condensate [22]. Zhang et.al. suggested that Raman or infrared spectroscopy can be used to observe the Fröhlich condensate in some modern proteins [17].

In this Letter, we report for the first time the Fröhlich condensate of phonons in a physical system. To do so, we realize the effective two-phonon-energy-redistribution

processes between different mechanical modes by placing an array of membranes in the middle of an optical cavity so that the interaction between the optical and mechanical mode is proportional to the square of the displacement. By making use of the adiabatic approximation, we can treat the optical field as a controllable reservoir [23, 24], which is quite different from the biological systems where the two-phonon processes are determined by the environment. Analytical and numerical methods show that the critical optomechanical coupling strength required to achieve the Fröhlich condensate scales as N^3 (N is the number of membranes). On the other hand, we find large N can dramatically suppress the decoherence of condensate.

Model and rate equations.— We consider a system consisting of a one-dimensional array of N membranes with the first membrane positioned in the middle of an optical cavity (see Fig. (1)). The cavity is pumped by a driving laser. In this configuration, the cavity field couples to the square of the displacement of the first membranes [25–28]. Thus, the optomechanical interaction ($\hbar = 1$) has the form $H_{om} = G\hat{a}^\dagger\hat{a}\hat{x}_1^2$, where \hat{a} (\hat{a}^\dagger) is the photon annihilation (creation) operator for the cavity mode with

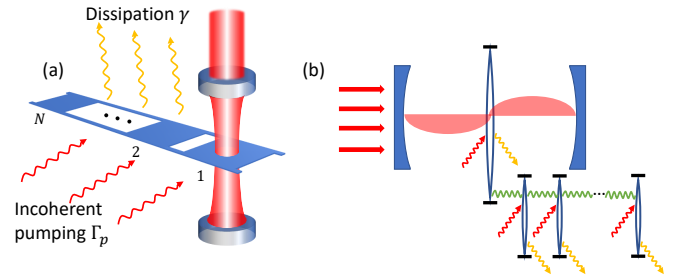


FIG. 1. (a) Schematic of an optomechanical system: an optical cavity interacting with a one-dimensional array of membranes. (b) Simplified model. The dissipation is due to the contact of the system with environment. The incoherent phonon pumping is not necessary for our system to get Fröhlich condensate, it is optional.

frequency ω_c , \hat{x}_1 is the position operator of the first membrane. The coupling strength $G = \omega_c''/2$ represents the frequency shift of the cavity mode induced by the square of displacement. The array of membranes is described by a chain of harmonic oscillators with nearest-neighbor coupling k . The mass of each oscillator is m .

In the frame rotating at the driving frequency ω_d , the system Hamiltonian can be simplified by the linearization of the cavity field ($\hat{a} = \bar{\alpha} + \hat{d}$) and diagonalization of the mechanical Hamiltonian. The system Hamiltonian in the eigenbasis of mechanical system is given by [29]

$$\hat{H} = -\Delta \hat{d}^\dagger \hat{d} + \sum_{j=1}^N \omega_j \hat{b}_j^\dagger \hat{b}_j + \frac{2g_0}{N+1} (\bar{\alpha} \hat{d}^\dagger + \bar{\alpha}^* \hat{d}) \times \left[\sum_j U_{j,j} (\hat{b}_j + \hat{b}_j^\dagger)^2 + \sum_{i<j} 2U_{i,j} (\hat{b}_i + \hat{b}_i^\dagger) (\hat{b}_j + \hat{b}_j^\dagger) \right], \quad (1)$$

where $\Delta = \omega_d - \omega_c$ is the detuning, $\omega_j^2 = \frac{k_0}{m} - \frac{2k}{m} \cos\left(\frac{j\pi}{N+1}\right)$ is the eigenfrequencies of the mechanical eigenmode, with annihilation (creation) operator given by \hat{b}_j (\hat{b}_j^\dagger), k_0 is the internal spring constant shifted by the cavity field. The optomechanical coupling is $g_0 = Gx_0^2$, with $x_0 = \sqrt{\hbar/(2m\omega_0)}$ and $\omega_0 = \sqrt{k_0/m}$. The coherent amplitude $\bar{\alpha}$ of the cavity field is given by $\bar{\alpha} = -iE/(\kappa/2 - i\Delta)$, where E is the amplitude of the driving laser and κ is the decay rate of the cavity field. The coefficient $U_{i,j} = \omega_0 \sin\left(\frac{i\pi}{N+1}\right) \sin\left(\frac{j\pi}{N+1}\right) / \sqrt{\omega_i \omega_j}$ comes from the diagonalization. The evolution of the system is governed by the quantum master equation,

$$\dot{\rho} = -i[\hat{H}, \rho] + \kappa \mathcal{D}[\hat{d}]\rho + \sum_{j=1}^N \left\{ \gamma_j (1 + \bar{n}_{j,\text{th}}) \mathcal{D}[\hat{b}_j]\rho + \gamma_j \bar{n}_{j,\text{th}} \mathcal{D}[\hat{b}_j^\dagger]\rho \right\}, \quad (2)$$

where ρ is the system density operator, \hat{H} is given by Eq. (1), κ and γ_j are the decay rate of the optical and the j th mechanical modes, respectively. $\bar{n}_{j,\text{th}}$ is the thermal phonon population of the j th mechanical mode, and $\mathcal{D}[\hat{o}]\rho = \hat{o}\rho\hat{o}^\dagger - \frac{1}{2}(\hat{o}^\dagger\hat{o}\rho + \rho\hat{o}^\dagger\hat{o})$ is the Lindblad term. Here we assume large optical dissipation $\kappa \gg \bar{n}_{j,\text{th}}\gamma_j$ and weak optomechanical coupling $\kappa, \omega_j \gg g_0|\bar{\alpha}|$. Hence, we can adiabatically eliminate the cavity field and get the master equation for the reduced density operator ρ_m of mechanical part [30]. The rate equations for the average phonon numbers derived from the reduced master equation are given by [29]

$$\begin{aligned} \langle \dot{\hat{n}}_l \rangle = & -\gamma_l (\langle \hat{n}_l \rangle - \bar{n}_{l,\text{th}}) \\ & + \sum_{j \neq l} 4U_{j,l}^2 [\Gamma(\omega_j - \omega_l) \langle (\hat{n}_l + 1) \hat{n}_j \rangle \\ & - \Gamma(\omega_l - \omega_j) \langle \hat{n}_l (\hat{n}_j + 1) \rangle]. \end{aligned} \quad (3)$$

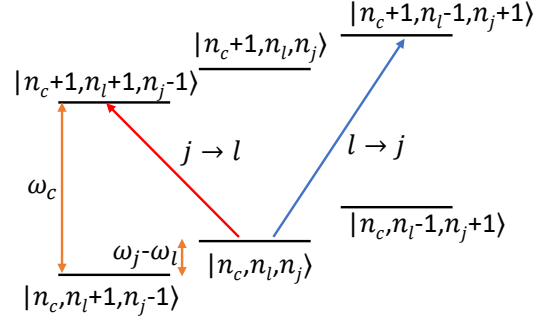


FIG. 2. Transition processes between the l th mode and the j th mode in the case of $\omega_l < \omega_j$. n_c , n_l and n_j represent the photon number, phonon number at the l th mode and the j th mode, respectively. The red arrow represents the second line of Eq. (3), which describes the process such that one phonon at the j th mode is pumped to the l th mode by the red-detuned driving laser. The blue arrow describes the reverse process pumped by the blue-detuned driving laser.

To close Eq. (3), we make the decorrelation approximation $\langle \hat{n}_l \hat{n}_j \rangle \approx \langle \hat{n}_l \rangle \langle \hat{n}_j \rangle$. On the right-hand side of Eq. (3), the first line describes the dissipation induced by the heat bath. The second line describes the absorption of a phonon with energy $\hbar\omega_j$ in conjunction with emission of a phonon with energy $\hbar\omega_l$, the third line describes the reverse processes, as illustrated in Fig. (2). The transition rates are governed by

$$\Gamma(\omega) = \frac{4g_0^2}{(N+1)^2} S_{nn}(\omega), \quad (4)$$

where $S_{nn}(\omega) = \frac{4\kappa|\bar{\alpha}|^2}{4(\omega+\Delta)^2 + \kappa^2}$ is the photon number spectral density. In the derivation of Eq. (3), we have neglected the sideband cooling and heating processes [29]. The validity of this approximation requires that the detuning satisfies $|\Delta| \approx |\omega_l - \omega_j|$, the frequency band is narrow ($|\omega_l - \omega_j| \ll \omega_l, \omega_j$) and the side-band cooling and heating processes are much weaker than the dissipation ($U_{l,l}^2 \Gamma(\pm 2\omega_l) \langle \hat{n}_l \rangle \ll \gamma_l$). All of these requirements are satisfied by the experimental parameters we used.

There are mainly two differences between Fröhlich's original model and Eq. (3): (i) the incoherent phonon pumping is optional in our scheme; (ii) the two-phonon-energy-redistribution processes can be controlled via the detuning and power of the driving laser in our scheme, while these processes are determined by the environment in Fröhlich's original model.

We assume that $\gamma_l = \gamma$, then the evolution of total phonon number ($\langle \hat{N}_{\text{tot}} \rangle = \sum_l \langle \hat{n}_l \rangle$) only depends on the dissipation processes. The steady state of $\langle \hat{N}_{\text{tot}} \rangle$ is given by $\langle \hat{N}_{\text{tot}} \rangle = \sum_l \langle \bar{n}_{l,\text{th}} \rangle$. In the case of $\langle \hat{n}_j \rangle \gg 1$, the net transition rate from the j th mode to the lowest mode is approximately given by

$$\Gamma_{j \rightarrow 1} = 4U_{j,1}^2 [\Gamma(\omega_j - \omega_1) - \Gamma(\omega_1 - \omega_j)] \langle \hat{n}_1 \rangle \langle \hat{n}_j \rangle. \quad (5)$$

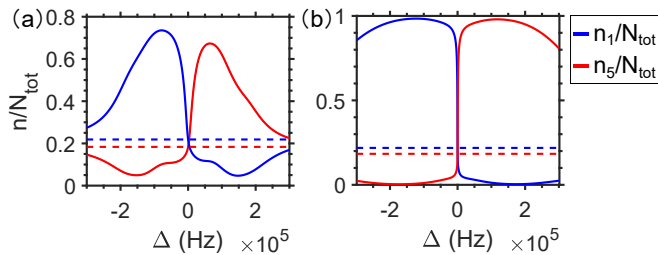


FIG. 3. The steady-state ratio of phonon numbers with respect to detuning. (a) The optomechanical coupling $g_0|\bar{\alpha}| = 10^{-5}\kappa$. (b) $g_0|\bar{\alpha}| = 5 \times 10^{-5}\kappa$. $N = 5$. The membrane and cavity parameters we use are close to those in Ref. [25, 26]. $\omega_0 = 1$ MHz, $\kappa = 100$ kHz, $\gamma = 0.1$ Hz, $T = 300$ mK, the thermal phonon population \bar{n}_{th} is at the order of 10^4 . The mechanical coupling is chosen as $k/m = \omega_0^2/10$. The blue (red) dashed line denotes the ratio of phonon numbers at the lowest (highest) mode in thermal equilibrium.

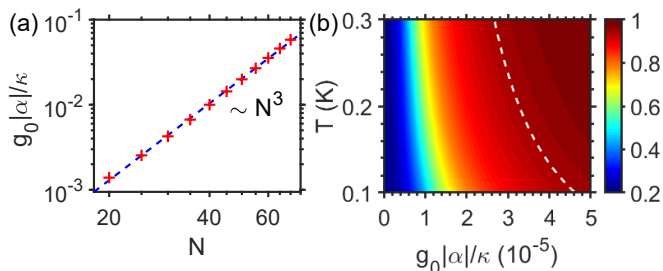


FIG. 4. Critical condition of Fröhlich condensate. (a) The minimum value of optomechanical coupling required to realize $a = 0.99$ with respect to the number of membranes. (b) The contour of $\langle \hat{n}_1 \rangle / \langle \hat{N}_{\text{tot}} \rangle$ in steady state with respect to $g_0|\bar{\alpha}|$ and temperature. The dashed line fitted by Eq. (6) agrees well with the contour lines $\langle \hat{n}_1 \rangle / \langle \hat{N}_{\text{tot}} \rangle = 0.945$. In (a) and (b), $\Delta = -k/(m\omega_0)$, the cavity and membrane parameters are fixed and are the same as those used in Fig. (3).

To realize Fröhlich condensate requires $\Gamma_{j \rightarrow 1}$ to be as large as possible. The rate $\Gamma_{j \rightarrow 1}$ can be increased by three approaches: (i) controlling the detuning Δ ; (ii) increasing the optomechanical couplings $g_0|\bar{\alpha}|$ by increasing the power of driving laser; (iii) increasing the phonon number $\langle \hat{n}_1 \rangle \langle \hat{n}_j \rangle$ by increasing the temperature or applying an external phonon pumping.

Dependence of condensation on experimental parameters.— From Eq. (5), we find $\Gamma_{j \rightarrow 1} > 0$ for red detuning ($\Delta < 0$). Similarly, we find the net transition rate from the j th mode to the highest mode is always positive ($\Gamma_{j \rightarrow N} > 0$) for blue detuning ($\Delta > 0$). Hence, phonons will concentrate at the lowest (highest) mode for red (blue) detuning. This analysis agrees with the simulations of steady-state ratio of average phonon numbers at the lowest and highest mode at different detuning, as shown in Fig. (3). The optimal detuning regime is $|\Delta| \sim k/(m\omega_0) = 10^5$ Hz, which is about one half of the frequency band. If the detuning is far

away from the optimal regime, the condensate no longer exists.

Besides the detuning, the realization of Fröhlich condensate is largely affected by the optomechanical couplings and temperature. Here we give an order of magnitude estimate of the critical condition. The starting point is the rate equation for the lowest mode (Eq. (3) in the case of $l = 1$). If the Fröhlich condensate is achieved, we can assume $\langle \hat{n}_1 \rangle = a \langle \hat{N}_{\text{tot}} \rangle$, where a is a number close to 1. For large N , we can obtain an estimate of the critical condition [29]

$$\frac{3000\pi^6(1-a)k\kappa|\Delta|g_0^2|\bar{\alpha}|^2\bar{n}_{\text{th}}}{m\omega_0\gamma(\kappa^2 + 4\Delta^2)^2} \sim N^6, \quad (6)$$

where we have chosen $\Delta = -k/(m\omega_0)$, $\bar{n}_{\text{th}} = \frac{1}{N} \sum_l \langle \bar{n}_{l,\text{th}} \rangle$ is the mean thermal phonon number. In the limit of $k_B T \gg \hbar\omega_0$, we have $\bar{n}_{\text{th}} \approx \frac{k_B T}{\hbar\omega_0}$, where k_B is the Boltzmann constant. Eq. (6) shows that the product of $g_0^2|\bar{\alpha}|^2$ and temperature T is proportional to N^6 . To verify our estimation, we plot the minimum value of $g_0|\bar{\alpha}|$ required to achieve a condensation with $a = 0.99$ and all other parameters fixed, as shown in Fig. (4a). It is seen that $g_0|\bar{\alpha}|$ is proportional to N^3 , which agrees well with our estimation. Fig. (4b) shows the contour of $\langle \hat{n}_1 \rangle / \langle \hat{N}_{\text{tot}} \rangle$ in steady state with respect to $g_0|\bar{\alpha}|$ and temperature. The dashed line is of the form $T = c_1/(g_0|\bar{\alpha}|)^2$, which agrees well with the contour line of $\langle \hat{n}_1 \rangle / \langle \hat{N}_{\text{tot}} \rangle$. Unlike the Fröhlich's model in which the critical pumping rate is proportional to $1/N$ [17], in our model the critical product of $g_0^2|\bar{\alpha}|^2$ and temperature T is proportional to N^6 . This makes the realization of Fröhlich condensate in large N -membrane systems challenging. The N^6 scaling is mainly due to the coefficient $1/(N+1)^2$ of the rate function $\Gamma(\omega)$ and the sine functions in $U_{j,l}$. To lower the requirements of implementing the Fröhlich condensate, we can introduce multiple cavities to couple more membranes. In addition, we can change the arrangement of the membranes to change the eigenmodes, e.g. instead of coupling in series like in Fig (1), parallel coupling can be used.

The incoherent phonon pumping in Fröhlich's original model can also be introduced to our system. The incoherent pumping can increase the phonon numbers in the system. If we assume the pumping rate is Γ_p , then the total phonon number in the system is $\langle N_{\text{tot}} \rangle = \frac{N\Gamma_p}{\gamma} + N\bar{n}_{\text{th}}$. We can introduce the effective temperature of the system $T_{\text{eff}} \approx T + \frac{\hbar\omega_0\Gamma_p}{k_B\gamma}$. By applying external phonon pumping, we can lower the required temperature and optomechanical coupling.

The coherence of Fröhlich condensate.— Another important property is the coherence of the Fröhlich condensate. As pointed out by Reimers et.al., high energy concentrated at the lowest mode does not ensure coherent vibrational motion [7].

To describe the coherence of the lowest mode, we

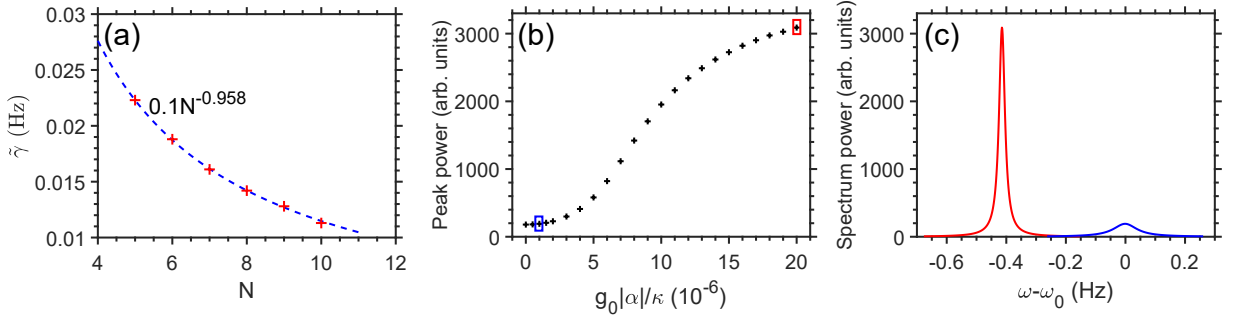


FIG. 5. The coherence of Fröhlich condensate. (a) The coherence decay rate of the lowest mode with respect to the number of membranes. $g_0|\bar{\alpha}|/\kappa$ are chosen to achieve $a = 0.99$. (b) The peak power of the phonon spectra of the lowest mode with respect to the optomechanical couplings. (c) The spectra at the optomechanical couplings indicated by the blue (red) rectangle in (b). In (b) and (c), $N = 5$. The cavity and membrane parameters in (a)-(c) are the same as those used in Fig. (3).

use the first-order correlation function $G^{(1)}(t, t + \tau) \propto \langle \hat{b}_1^\dagger(t) \hat{b}_1(t + \tau) \rangle$. The coherence of the condensate is characterized by the decay rate $\tilde{\gamma}(t)$ of $G^{(1)}(t, t + \tau)$. At the long-time limit, $\tilde{\gamma}(t)$ can be simplified as [29]

$$\begin{aligned} \tilde{\gamma} &= \frac{\gamma \bar{n}_{1,\text{th}}}{\langle \hat{n}_1 \rangle} \\ &+ 2U_{1,1}^2 \left[\Gamma(2\omega_1) + \Gamma(-2\omega_1) \left(1 + \frac{2}{\langle \hat{n}_1 \rangle} \right) + \Gamma(0) \right] \\ &+ \sum_{j=2}^N 4U_{j,1}^2 \left[\Gamma(-\omega_1 - \omega_j) \frac{\langle \hat{n}_j \rangle}{\langle \hat{n}_1 \rangle} + \Gamma(\omega_j - \omega_1) \frac{\langle \hat{n}_j + 1 \rangle}{\langle \hat{n}_1 \rangle} \right]. \end{aligned} \quad (7)$$

The term in the first line is at the order of γ/N . For the rest of terms, the maximum order of magnitude is about $\frac{m\omega_0\gamma(\kappa^2 + 4\Delta^2)}{10\pi^2 ak|\Delta|\bar{n}_{\text{th}}}$ when Eq. (6) is satisfied. Thus $\tilde{\gamma}$ is mainly determined by the first term when $N \ll \frac{10\pi^2 ak|\Delta|\bar{n}_{\text{th}}}{m\omega_0(\kappa^2 + 4\Delta^2)}$. If we use the experimental parameters in Fig. (3) and $a = 0.99$, it is about $N \ll 10^6$. In this case, the coherence of the lowest mode is approximately given by

$$\tilde{\gamma} \approx \frac{\gamma \bar{n}_{1,\text{th}}}{\langle \hat{n}_1 \rangle} \approx \frac{\gamma}{N}, \quad (8)$$

Eq. (8) shows that the decoherence of Fröhlich condensate can be largely suppressed by increasing the number of membranes in the system. Recall the uncertainty relations for the number of photons and the phase of a laser mode $\delta\varphi \sim 1/\langle n \rangle$, we find the Fröhlich condensate in our scheme is like a laser. To verify our prediction, we simulate the long-time evolution of the correlation function and calculate the spectral density

$$S_{\text{cor}}(\omega) \propto \lim_{t \rightarrow \infty} \int_0^\infty d\tau e^{i\omega\tau} \langle \hat{b}_1^\dagger(t) \hat{b}_1(t + \tau) \rangle. \quad (9)$$

The coherence decay rate is determined by the full width at half maximum (FWHM) of the spectra. Fig. (5a) illustrates the coherence decay rate $\tilde{\gamma}$ with respect to various

numbers of membranes. The fitted line agrees well with Eq. (8). The long-lived coherence of the Fröhlich condensate in optomechanical system makes it a potential platform to realize a narrow-linewidth phonon laser [31, 32]. Fig. (5b) shows the peak power of the phonon spectra of the lowest mode versus optomechanical couplings. At small $g_0|\bar{\alpha}|$, the peak power is small and increases slowly with $g_0|\bar{\alpha}|$. At intermediate $g_0|\bar{\alpha}|$, the peak power increases quickly. At large $g_0|\bar{\alpha}|$, the peak power tends to saturate, which corresponds to the condition where almost all phonons occupy the lowest mode. Fig. (5c) shows line narrowing and power increasing of the spectra with the increase of $g_0|\bar{\alpha}|$, which demonstrates the formation of phonon lasing.

Discussion and conclusion.— Here we estimate the experimental feasibility of Fröhlich condensate by using existing available systems. We use the membrane and cavity parameters of Ref. [26]. The mechanical array is composed of $1 \text{ mm} \times 1 \text{ mm} \times 50 \text{ nm}$ Si_3N_4 membranes with resonance at $\omega_0 = 2\pi \times 134 \text{ kHz}$ and mass $m = 40 \text{ ng}$. The cavity allows the existence of many transverse electromagnetic (TEM) modes. The TEM_{00} mode of the cavity has a decay rate $\kappa = 300 \text{ kHz}$. The cavity is excited by a laser with wavelength $\lambda = 1064 \text{ nm}$. The coupling between mechanical mode and TEM_{00} mode at the TEM_{02} - TEM_{00} crossing can be as large as $G = \omega_c''/2 = 2\pi \times 15 \text{ MHz}\cdot\text{nm}^{-2}$. The corresponding coupling is $g_0 = Gx_0^2 = 1.5 \times 10^{-4} \text{ Hz}$. At $T = 300 \text{ mK}$, the Q factor of the membrane is $Q_m = 1.2 \times 10^7$, which corresponds to the decay rate $\gamma = 0.07 \text{ Hz}$. We assume the coupling between membranes is $k/m = \omega_0^2/10$, the detuning is $\Delta = -k/(m\omega_0)$ and the number of membranes is $N = 5$. Using Eq. (6), we get the coherent amplitude $|\bar{\alpha}|$ of the cavity field required to achieve $\langle n_1 \rangle / \langle N_{\text{tot}} \rangle = 0.99$ is $|\bar{\alpha}| = 1.6 \times 10^4$. According to the formula $\bar{\alpha} = -iE/(\kappa/2 - i\Delta)$ and $E = \sqrt{\frac{\kappa P_{\text{in}}}{\hbar\omega_d}}$, the required laser power is $P_{\text{in}} \approx 5 \mu\text{W}$. This is feasible in nowadays lab. The mechanical membrane is scalable. A further analysis of experimental feasibility in different

membranes sizes can be found in Ref. [29].

Besides the setup in Fig. (1), we can also consider quadratically coupling the multiple modes of a single membranes to the cavity. In experiment, the linear interaction between multiple mechanical modes of a membrane and an optical mode has been reported [33]. With a much larger quadratic coupling strength $g_0|\bar{\alpha}|/\kappa \approx 1$ [34, 35], the optomechanical interaction between ultracold atomic gas and cavity can be a candidate to realize Fröhlich condensate as well.

In conclusion, we have proposed that the Fröhlich condensate can be realized in an array of mechanical membranes coupled to an optical cavity. Compared to the biological systems studied before, the optomechanical system can be well controlled by the driving laser [36, 37]. The numerical results show that the optimal detuning of driving laser is around $|\Delta| \sim k/(m\omega_0)$. The coherence lifetime of Fröhlich condensate is proportional to the number of membranes, which can be further improved by increasing the number of membranes. On the other hand, large number of membranes greatly increases the required optomechanical coupling strength and temperature ($g_0|\bar{\alpha}|^2T \propto N^6$). The possible solutions to lower the requirement include coupling more membranes to the optical cavities or changing the arrangement of membranes.

Fröhlich condensates in optomechanical systems have potential applications in generating narrow-linewidth phonon laser. Our scheme can be extended to electromechanical system [38], which sheds light on the design of novel acoustic transducer to generate coherent and single frequency sound. Moreover, our scheme is likely to be used in the energy conversion and transfer, frequency filter, heat control [39, 40], etc. By switching the role of phonon and photon, we may realize the Fröhlich-like photon condensate, which may be used in acoustic-induced-optical lasing. Since most phonons occupy the lowest mode in the Fröhlich condensate, we may realize the efficient multimode cooling of mechanical oscillators by adding another laser to cool the lowest mode.

* Xu.Zheng@Colorado.Edu

† Baowen.Li@Colorado.Edu

- [1] R. Bonifacio and L. Lugiato, Phys. Rev. A **11**, 1507 (1975).
- [2] A. Pikovsky, M. Rosenblum, and J. Kurths, *Synchronization: a universal concept in nonlinear sciences*, Vol. 12 (Cambridge University Press, 2003).
- [3] G. Heinrich, M. Ludwig, J. Qian, B. Kubala, and F. Marquardt, Phys. Rev. Lett. **107**, 043603 (2011).
- [4] M. Zhang, S. Shah, J. Cardenas, and M. Lipson, Phys. Rev. Lett. **115**, 163902 (2015).
- [5] M. F. Colombano, G. Arregui, N. E. Capuj, A. Pitanti, J. Maire, A. Griol, B. Garrido, A. Martínez, C. M. Sotomayor-Torres, and D. Navarro-Urrios, Phys. Rev. Lett. **123**, 017402 (2019).
- [6] J. Sheng, X. Wei, C. Yang, and H. Wu, Phys. Rev. Lett. **124**, 053604 (2020).
- [7] J. R. Reimers, L. K. McKemmish, R. H. McKenzie, A. E. Mark, and N. S. Hush, Proc. Nat. Acad. Sci. **106**, 4219 (2009).
- [8] S. Hameroff and R. Penrose, Phys. Life Rev. **11**, 39 (2014).
- [9] H. Fröhlich, Inter. J. of Quant. Chem. **2**, 641 (1968).
- [10] H. Fröhlich, Phys. Lett. A **26**, 402 (1968).
- [11] H. Fröhlich, Nature **228**, 1093 (1970).
- [12] K. B. Davis, M.-O. Mewes, M. R. Andrews, N. J. van Druten, D. S. Durfee, D. Kurn, and W. Ketterle, Phys. Rev. Lett. **75**, 3969 (1995).
- [13] D. Jin, J. Ensher, M. Matthews, C. Wieman, and E. A. Cornell, Phys. Rev. Lett. **77**, 420 (1996).
- [14] T. Wu and S. Austin, Phys. Lett. A **64**, 151 (1977).
- [15] T. Wu and S. Austin, Phys. Lett. A **65**, 74 (1978).
- [16] T. Wu and S. J. Austin, J Biol. Phys. **9**, 97 (1981).
- [17] Z. Zhang, G. S. Agarwal, and M. O. Scully, Phys. Rev. Lett. **122**, 158101 (2019).
- [18] S. O. Demokritov, V. E. Demidov, O. Dzyapko, G. A. Melkov, A. A. Serga, B. Hillebrands, and A. N. Slavin, Nature **443**, 430 (2006).
- [19] A. Chumak, G. Melkov, V. Demidov, O. Dzyapko, V. Safonov, and S. Demokritov, Phys. Rev. Lett. **102**, 187205 (2009).
- [20] O. Misochko, M. Hase, K. Ishioka, and M. Kitajima, Phys. Lett. A **321**, 381 (2004).
- [21] I. Altfeder, A. A. Voevodin, M. H. Check, S. M. Eichfeld, J. A. Robinson, and A. V. Balatsky, Sci. Rep **7**, 1 (2017).
- [22] I. Nardecchia, J. Torres, M. Lechelon, V. Giliberti, M. Ortolani, P. Nouvel, M. Gori, Y. Meriguet, I. Donato, J. Preto, *et al.*, Phys. Rev. X **8**, 031061 (2018).
- [23] A. Tomadin, S. Diehl, M. D. Lukin, P. Rabl, and P. Zoller, Phys. Rev. A **86**, 033821 (2012).
- [24] J. H. Lee and H. Seok, Phys. Rev. A **97**, 013805 (2018).
- [25] J. Thompson, B. Zwickl, A. Jayich, F. Marquardt, S. Girvin, and J. Harris, Nature **452**, 72 (2008).
- [26] J. C. Sankey, C. Yang, B. M. Zwickl, A. M. Jayich, and J. G. Harris, Nat. Phys. **6**, 707 (2010).
- [27] J.-Q. Liao, F. Nori, *et al.*, Phys. Rev. A **88**, 023853 (2013).
- [28] J.-Q. Liao and F. Nori, Sci. Rep. **4**, 1 (2014).
- [29] See Supplemental Material for details.
- [30] H. J. Carmichael, *Statistical methods in quantum optics 1: master equations and Fokker-Planck equations* (Springer Science & Business Media, 2013).
- [31] I. S. Grudinin, H. Lee, O. Painter, and K. J. Vahala, Phys. Rev. Lett. **104**, 083901 (2010).
- [32] H. Jing, S. Özdemir, X.-Y. Lü, J. Zhang, L. Yang, and F. Nori, Phys. Rev. Lett. **113**, 053604 (2014).
- [33] W. H. P. Nielsen, Y. Tsaturyan, C. B. Møller, E. S. Polzik, and A. Schliesser, Proc. Natl. Acad. Sci. **114**, 62 (2017).
- [34] K. W. Murch, K. L. Moore, S. Gupta, and D. M. Stamper-Kurn, Nature Physics **4**, 561 (2008).
- [35] T. P. Purdy, D. Brooks, T. Botter, N. Brahms, Z.-Y. Ma, and D. M. Stamper-Kurn, Phys. Rev. Lett. **105**, 133602 (2010).
- [36] T. J. Kippenberg and K. J. Vahala, Science **321**, 1172 (2008).
- [37] M. Aspelmeyer, T. J. Kippenberg, and F. Marquardt, Rev. Mod. Phys. **86**, 1391 (2014).

- [38] X. Ma, J. J. Viennot, S. Kotler, J. D. Teufel, and K. W. Lehnert, *Nature Physics* (2021).
- [39] A. Seif, W. DeGottardi, K. Esfarjani, and M. Hafezi, *Nature Communications* **9**, 1 (2018).
- [40] C. Yang, X. Wei, J. Sheng, and H. Wu, *Nature Communications* **11**, 1 (2020).

Fröhlich Condensate of Phonons in Optomechanical Systems: Supplementary Material

Xu Zheng^{1,*} and Baowen Li^{2,1,†}

¹*Department of Physics, University of Colorado, Boulder, CO, 80309, USA*

²*Paul M. Rady Department of Mechanical Engineering,
University of Colorado, Boulder, CO, 80309, USA*

(Dated: February 28, 2025)

This supplementary material gives the derivations for some equations in the main text and more numerical results in support of the main text.

SYSTEM HAMILTONIAN IN MECHANICAL EIGENMODES

We consider a system consisting of a one-dimensional array of N membranes with the first membrane coupled to a cavity field. The first membrane is positioned near a node (or antinode) of the standing light wave that forms one optical mode so that the cavity field couples to the square of the displacement [1, 2], as shown in the Fig. (1) of the main text. The Hamiltonian for this system ($\hbar = 1$) is

$$\hat{H}_0 = \omega_c \hat{a}^\dagger \hat{a} + E(\hat{a}^\dagger e^{-i\omega_d t} + \hat{a} e^{i\omega_d t}) + \sum_{j=1}^N \left(\frac{\hat{p}_j^2}{2m} + \frac{1}{2} k_j \hat{x}_j^2 \right) - \sum_{j=1}^{N-1} k \hat{x}_j \hat{x}_{j+1} + G \hat{a}^\dagger \hat{a} \hat{x}_1^2, \quad (\text{S1})$$

where \hat{a} (\hat{a}^\dagger) is the photon annihilation (creation) operator, ω_c is the frequency of the cavity mode, ω_d is the frequency of the coherent driving field with amplitude E . The array of membranes is described by a chain of harmonic oscillators with nearest-neighbor coupling. \hat{p}_j (\hat{x}_j) is the momentum (displacement) operator of the j th membrane, k_j is the internal spring constant of the j th membrane, and the nearest-neighbor coupling between membranes is k . Here we have assumed the coupling is the same for all nearest membranes and all membranes have the same mass m . The optomechanical coupling strength $G = \omega_c''/2$ represents the frequency shift of the cavity mode induced by the square of displacement.

It is convenient to switch to a frame rotating at the driving frequency ω_d . Applying the unitary transformation $\hat{U} = \exp(-i\omega_d \hat{a}^\dagger \hat{a} t)$ generates the new Hamiltonian

$$\hat{H}' = -\Delta \hat{a}^\dagger \hat{a} + E(\hat{a}^\dagger + \hat{a}) + \sum_{j=1}^N \left(\frac{\hat{p}_j^2}{2m} + \frac{1}{2} k_j \hat{x}_j^2 \right) - \sum_{j=1}^{N-1} k \hat{x}_j \hat{x}_{j+1} + G \hat{a}^\dagger \hat{a} \hat{x}_1^2, \quad (\text{S2})$$

where $\Delta = \omega_d - \omega_c$ is the detuning. Splitting the cavity field into an average coherent amplitude and a fluctuating term $\hat{a} = \bar{\alpha} + \hat{d}$, and neglecting $\hat{d}^\dagger \hat{d}$ with respect to $(\bar{\alpha} \hat{d}^\dagger + \bar{\alpha}^* \hat{d})$, we obtain the following Hamiltonian

$$\hat{H} = -\Delta \hat{d}^\dagger \hat{d} + \sum_{j=1}^N \left(\frac{\hat{p}_j^2}{2m} + \frac{1}{2} k'_j \hat{x}_j^2 \right) - \sum_{j=1}^{N-1} k \hat{x}_j \hat{x}_{j+1} + G(\bar{\alpha} \hat{d}^\dagger + \bar{\alpha}^* \hat{d}) \hat{x}_1^2, \quad (\text{S3})$$

where $k'_j = k_j + 2G|\bar{\alpha}|^2 \delta_{j,1}$ is the shifted internal spring constant, the coherent amplitude $\bar{\alpha}$ is given by

$$\bar{\alpha} = \frac{-iE}{\kappa/2 - i\Delta}, \quad (\text{S4})$$

where κ is the decay rate of the cavity mode. For simplicity, we assume that $k'_j = k_0$. The mechanical part in Eq. (S3) can be diagonalized with the well-known eigenfrequencies and eigenmodes

$$\omega_j^2 = \frac{k_0}{m} - \frac{2k}{m} \cos\left(\frac{j\pi}{N+1}\right), \quad \mathbf{Y} = \mathbf{M}\mathbf{X}, \quad M_{i,j} = \sqrt{\frac{2}{N+1}} \sin\left(\frac{ij\pi}{N+1}\right), \quad (\text{S5})$$

* Xu.Zheng@Colorado.Edu

† Baowen.Li@Colorado.Edu

where $\mathbf{Y} = [\hat{y}_1, \hat{y}_2, \dots, \hat{y}_N]^T$, $\mathbf{X} = [\hat{x}_1, \hat{x}_2, \dots, \hat{x}_N]^T$. The Hamiltonian in the new basis is

$$\hat{H} = -\Delta \hat{d}^\dagger \hat{d} + \sum_{j=1}^N \left(\frac{\hat{p}_{y,j}^2}{2m} + \frac{1}{2} m \omega_j^2 \hat{y}_j^2 \right) + G(\bar{\alpha} \hat{d}^\dagger + \bar{\alpha}^* \hat{d}) \left(\sum_{j=1}^N M_{j1} \hat{y}_j \right)^2. \quad (\text{S6})$$

Introducing the phonon creation (\hat{b}_j^\dagger) and annihilation (\hat{b}_j) operators, with

$$\hat{y}_j = \sqrt{\frac{\hbar}{2m\omega_j}} (\hat{b}_j^\dagger + \hat{b}_j), \quad \hat{p}_{y,j} = -i\sqrt{\frac{\hbar m \omega_j}{2}} (\hat{b}_j^\dagger - \hat{b}_j), \quad (\text{S7})$$

we obtain the Hamiltonian

$$\hat{H} = -\Delta \hat{d}^\dagger \hat{d} + \sum_{j=1}^N \omega_j \hat{b}_j^\dagger \hat{b}_j + \frac{2g_0}{N+1} (\bar{\alpha} \hat{d}^\dagger + \bar{\alpha}^* \hat{d}) \left[\sum_j U_{j,j} (\hat{b}_j + \hat{b}_j^\dagger)^2 + \sum_{i<j} 2U_{i,j} (\hat{b}_i + \hat{b}_i^\dagger) (\hat{b}_j + \hat{b}_j^\dagger) \right], \quad (\text{S8})$$

where $g_0 = Gx_0^2$, with $x_0 = \sqrt{\hbar/(2m\omega_0)}$, $\omega_0 = \sqrt{k_0/m}$. And $U_{i,j}$ is given by

$$U_{i,j} = \frac{\omega_0 \sin\left(\frac{i\pi}{N+1}\right) \sin\left(\frac{j\pi}{N+1}\right)}{\sqrt{\omega_i \omega_j}}. \quad (\text{S9})$$

The Hamiltonian Eq. (S8) is the Eq. (1) in the main text.

QUANTUM MASTER EQUATIONS AND RATE EQUATIONS FOR PHONON NUMBERS

To derive the effective quantum master equations involving only the mechanical degrees of freedom, we can adiabatically eliminate the optical degrees of freedom. The validity of adiabatic elimination relies on two approximations: (i) the optical decay rate is much larger than the mechanical dissipation rate, i.e. the optical processes are much faster than mechanical processes. (ii) the optomechanical coupling is weak. The master equation for the system density operator ρ is given by

$$\begin{aligned} \dot{\rho} &= \mathcal{L}_o \rho + \mathcal{L}_m \rho + \mathcal{L}_{om} \rho \\ \mathcal{L}_o &= -i[-\Delta \hat{d}^\dagger \hat{d}, \cdot] + \kappa \mathcal{D}[\hat{d}] \\ \mathcal{L}_m &= \sum_{j=1}^N \left\{ -i[\omega_j \hat{b}_j^\dagger \hat{b}_j, \cdot] + \gamma_j (1 + \bar{n}_{j,\text{th}}) \mathcal{D}[\hat{b}_j] + \gamma_j \bar{n}_{j,\text{th}} \mathcal{D}[\hat{b}_j^\dagger] \right\} \\ \mathcal{L}_{om} &= -i[\hat{H}_{om}, \cdot]. \end{aligned} \quad (\text{S10})$$

where \hat{H}_{om} is the optomechanical coupling in Eq. (S8), κ and γ_j are the decay rate of the optical and the j th mechanical modes, respectively. $\bar{n}_{j,\text{th}}$ is the thermal phonon population of the j th mechanical mode, and $\mathcal{D}[\hat{o}]\rho = \hat{o}\rho\hat{o}^\dagger - \frac{1}{2}(\hat{o}^\dagger\hat{o}\rho + \rho\hat{o}^\dagger\hat{o})$ is the Lindblad term.. In the interaction picture, we transform the density operator as

$$\rho^I(t) = e^{-(\mathcal{L}_o + \mathcal{L}_m)t} \rho. \quad (\text{S11})$$

Then the master equation is transformed as

$$\dot{\rho}^I = \mathcal{L}_{om}^I(t) \rho^I, \quad (\text{S12})$$

with

$$\mathcal{L}_{om}^I(t) = e^{-(\mathcal{L}_o + \mathcal{L}_m)t} \mathcal{L}_{om} e^{(\mathcal{L}_o + \mathcal{L}_m)t}. \quad (\text{S13})$$

The formal solution of Eq. (S12) is given by

$$\rho^I(t) = \rho^I(0) + \int_0^t dt_1 \mathcal{L}_{om}^I(t_1) \rho^I(t_1). \quad (\text{S14})$$

Substituting the formal solution back into Eq. (S12) gives

$$\dot{\rho}^I = \mathcal{L}_{om}^I(t)\rho^I(0) + \int_0^t dt_1 \mathcal{L}_{om}^I(t)\mathcal{L}_{om}^I(t_1)\rho^I(t_1). \quad (\text{S15})$$

We assume that no correlations exist between the optical and mechanical field at $t = 0$. Then $\rho^I(0) = \rho(0) = \rho_o(0) \otimes \rho_m(0)$. Taking the partial trace over the optical degrees of freedom results in

$$\dot{\rho}_m^I = \int_0^t dt_1 \text{Tr}_o \{ \mathcal{L}_{om}^I(t)\mathcal{L}_{om}^I(t_1)\rho^I(t_1) \}, \quad (\text{S16})$$

where, for simplicity, we have eliminated the term $\text{Tr}_o \{ \mathcal{L}_{om}^I(t)\rho^I(0) \}$ with the assumption $\text{Tr}_o \{ \hat{d}\rho_o(0) \} = \text{Tr}_o \{ \hat{d}^\dagger\rho_o(0) \} = 0$. Since the optomechanical coupling is weak, the density operator can be written as

$$\rho^I(t) = \rho_o^I(t) \otimes \rho_m^I(t) + O(\hat{H}_{om}). \quad (\text{S17})$$

Now we make the standard Born-Markov approximation, the master equation for the reduced density operator is

$$\dot{\rho}_m^I = \int_0^t dt_1 \text{Tr}_o \{ \mathcal{L}_{om}^I(t)\mathcal{L}_{om}^I(t_1)\rho_o^I(t) \otimes \rho_m^I(t) \}. \quad (\text{S18})$$

The form of \hat{H}_{om} is

$$\hat{H}_{om} = \epsilon \hat{A} \hat{B}, \quad (\text{S19})$$

with

$$\begin{aligned} \epsilon &= \frac{2g_0}{N+1} \\ \hat{A} &= (\bar{\alpha}\hat{d}^\dagger + \bar{\alpha}^*\hat{d}) \\ \hat{B} &= \sum_i U_{i,i}(\hat{b}_i + \hat{b}_i^\dagger)^2 + \sum_{i<j} 2U_{i,j}(\hat{b}_i + \hat{b}_i^\dagger)(\hat{b}_j + \hat{b}_j^\dagger). \end{aligned} \quad (\text{S20})$$

Then the master equation is now

$$\begin{aligned} \dot{\rho}_m^I &= -\epsilon^2 \int_0^t dt_1 \left\{ (\hat{B}\cdot)_t (\hat{B}\cdot)_{t_1} \rho_m^I(t) \text{Tr}_o \left[(\hat{A}\cdot)_t (\hat{A}\cdot)_{t_1} \rho_o^I(t) \right] - (\hat{B}\cdot)_t (\cdot\hat{B})_{t_1} \rho_m^I(t) \text{Tr}_o \left[(\hat{A}\cdot)_t (\hat{A}\cdot)_{t_1} \rho_o^I(t) \right] \right. \\ &\quad \left. - (\hat{B}\cdot)_t (\hat{B}\cdot)_{t_1} \rho_m^I(t) \text{Tr}_o \left[(\hat{A}\cdot)_t (\hat{A}\cdot)_{t_1} \rho_o^I(t) \right] + (\cdot\hat{B})_t (\cdot\hat{B})_{t_1} \rho_m^I(t) \text{Tr}_o \left[(\hat{A}\cdot)_t (\hat{A}\cdot)_{t_1} \rho_o^I(t) \right] \right\}, \end{aligned} \quad (\text{S21})$$

where $(\hat{O}\cdot)_t = e^{-(\mathcal{L}_o + \mathcal{L}_m)t}(\hat{O}\cdot)e^{(\mathcal{L}_o + \mathcal{L}_m)t}$ and $(\cdot\hat{O})_t = e^{-(\mathcal{L}_o + \mathcal{L}_m)t}(\cdot\hat{O})e^{(\mathcal{L}_o + \mathcal{L}_m)t}$ are the operators in the interaction picture. The dot represents where the density operator is. Taking the time derivative on both sides, we obtain the equation satisfied by the optical operator $(\hat{d}\cdot)_t, (\cdot\hat{d})_t$:

$$\frac{d(\hat{d}\cdot)_t}{dt} = [(\hat{d}\cdot)_t, \mathcal{L}_o], \quad \frac{d(\cdot\hat{d})_t}{dt} = [(\cdot\hat{d})_t, \mathcal{L}_o]. \quad (\text{S22})$$

From Eq. (S22) we can obtain the explicit solutions

$$(\hat{d}\cdot)_t = e^{(i\Delta - \frac{\kappa}{2})t}(\hat{d}\cdot), \quad (\hat{d}^\dagger\cdot)_t = e^{-(i\Delta - \frac{\kappa}{2})t}(\hat{d}^\dagger\cdot) - e^{-(i\Delta + \frac{\kappa}{2})t}(e^{\kappa t} - 1)(\cdot\hat{d}^\dagger). \quad (\text{S23})$$

For the mechanical operators $(\hat{b}_j\cdot)_t$ and $(\hat{b}_j^\dagger\cdot)_t$ in the interaction picture, we have

$$(\hat{b}_j\cdot)_t = e^{-i\omega_j t}(\hat{b}_j\cdot), \quad (\hat{b}_j^\dagger\cdot)_t = e^{i\omega_j t}(\hat{b}_j^\dagger\cdot), \quad (\text{S24})$$

with the assumption that $\omega_j \gg \gamma_j$. We have assumed that $\kappa \gg \bar{n}_{j,\text{th}}\gamma_j, g_0|\bar{\alpha}|$, i.e., the time scale of mechanical dynamics is much larger than that of optical dynamics. Then $\rho_o^I(t) \approx \rho_o^I(\infty)$. Making use of Eq. (S23), we can obtain

$$\begin{aligned} \text{Tr}_o \left[(\hat{A}\cdot)_t (\hat{A}\cdot)_{t_1} \rho_o^I(t) \right] &= \text{Tr}_o \left[(\cdot\hat{A})_t (\hat{A}\cdot)_{t_1} \rho_o^I(t) \right] = |\bar{\alpha}|^2 e^{(i\Delta - \frac{\kappa}{2})(t-t_1)}, \\ \text{Tr}_o \left[(\hat{A}\cdot)_t (\cdot\hat{A})_{t_1} \rho_o^I(t) \right] &= \text{Tr}_o \left[(\cdot\hat{A})_t (\cdot\hat{A})_{t_1} \rho_o^I(t) \right] = |\bar{\alpha}|^2 e^{-(i\Delta + \frac{\kappa}{2})(t-t_1)}. \end{aligned} \quad (\text{S25})$$

From Eqs. (S24)-(S25), and neglecting the fast-oscillating terms, we can simplify the master equation Eq. (S21):

$$\begin{aligned}
\dot{\rho}_m^I &= \tilde{\mathcal{L}}\rho_m^I(t), \\
\tilde{\mathcal{L}} &= -i \sum_i U_{i,i}^2 \left[\tilde{\Delta}(2\omega_i)\hat{b}_i^\dagger\hat{b}_i^\dagger\hat{b}_i\hat{b}_i + \tilde{\Delta}(-2\omega_i)\hat{b}_i\hat{b}_i\hat{b}_i^\dagger\hat{b}_i^\dagger + \tilde{\Delta}(0)(\hat{b}_i^\dagger\hat{b}_i + \hat{b}_i\hat{b}_i^\dagger)^2, \cdot \right] \\
&\quad - i \sum_{i<j} 4U_{i,j}^2 \left[\tilde{\Delta}(\omega_i + \omega_j)\hat{b}_i^\dagger\hat{b}_j^\dagger\hat{b}_j\hat{b}_i + \tilde{\Delta}(-\omega_i - \omega_j)\hat{b}_i\hat{b}_j\hat{b}_j^\dagger\hat{b}_i^\dagger + \tilde{\Delta}(\omega_i - \omega_j)\hat{b}_i^\dagger\hat{b}_j\hat{b}_j^\dagger\hat{b}_i + \tilde{\Delta}(\omega_j - \omega_i)\hat{b}_i\hat{b}_j^\dagger\hat{b}_j\hat{b}_i^\dagger, \cdot \right] \\
&\quad + \sum_i U_{i,i}^2 \left\{ \Gamma(2\omega_i)\mathcal{D}[\hat{b}_i\hat{b}_i] + \Gamma(-2\omega_i)\mathcal{D}[\hat{b}_i^\dagger\hat{b}_i^\dagger] + \Gamma(0)\mathcal{D}[\hat{b}_i^\dagger\hat{b}_i + \hat{b}_i\hat{b}_i^\dagger] \right\} \\
&\quad + \sum_{i<j} 4U_{i,j}^2 \left\{ \Gamma(\omega_i + \omega_j)\mathcal{D}[\hat{b}_i\hat{b}_j] + \Gamma(-\omega_i - \omega_j)\mathcal{D}[\hat{b}_i^\dagger\hat{b}_j^\dagger] + \Gamma(\omega_i - \omega_j)\mathcal{D}[\hat{b}_i\hat{b}_j^\dagger] + \Gamma(\omega_j - \omega_i)\mathcal{D}[\hat{b}_i^\dagger\hat{b}_j] \right\}, \quad (\text{S26})
\end{aligned}$$

where the energy shift $\tilde{\Delta}(\omega)$ and the rate $\Gamma(\omega)$ are given by

$$\tilde{\Delta}(\omega) = \text{Im}[G(\omega)], \quad \Gamma(\omega) = 2\text{Re}[G(\omega)], \quad (\text{S27})$$

and $G(\omega)$ is the Fourier transform of the photon correlation function.

$$G(\omega) = \epsilon^2|\bar{\alpha}|^2 \int_0^t d\tau e^{i\omega\tau} e^{(i\Delta - \frac{\kappa}{2})\tau}. \quad (\text{S28})$$

Since τ integration is dominated by the times $\sim \kappa^{-1}$, which is much shorter than t , we can extend the τ integration to infinity,

$$G(\omega) = \epsilon^2|\bar{\alpha}|^2 \int_0^\infty d\tau e^{i\omega\tau} e^{(i\Delta - \frac{\kappa}{2})\tau} = \frac{\epsilon^2|\bar{\alpha}|^2}{-i(\Delta + \omega) + \kappa/2}. \quad (\text{S29})$$

Note that $\rho_m^I(t)$ is still in the interaction picture. Transforming back to $\rho_m(t)$ we obtain

$$\begin{aligned}
\dot{\rho}_m &= \mathcal{L}_m\rho_m + \tilde{\mathcal{L}}\rho_m \\
&= -i[\tilde{H}, \rho_m] + \sum_i \left\{ \gamma_i(1 + \bar{n}_{i,\text{th}})\mathcal{D}[\hat{b}_i] + \gamma_i\bar{n}_{i,\text{th}}\mathcal{D}[\hat{b}_i^\dagger] \right\} \rho_m \\
&\quad + \sum_i U_{i,i}^2 \left\{ \Gamma(2\omega_i)\mathcal{D}[\hat{b}_i\hat{b}_i] + \Gamma(-2\omega_i)\mathcal{D}[\hat{b}_i^\dagger\hat{b}_i^\dagger] + \Gamma(0)\mathcal{D}[\hat{b}_i^\dagger\hat{b}_i + \hat{b}_i\hat{b}_i^\dagger] \right\} \rho_m \\
&\quad + \sum_{i<j} 4U_{i,j}^2 \left\{ \Gamma(\omega_i + \omega_j)\mathcal{D}[\hat{b}_i\hat{b}_j] + \Gamma(-\omega_i - \omega_j)\mathcal{D}[\hat{b}_i^\dagger\hat{b}_j^\dagger] + \Gamma(\omega_i - \omega_j)\mathcal{D}[\hat{b}_i\hat{b}_j^\dagger] + \Gamma(\omega_j - \omega_i)\mathcal{D}[\hat{b}_i^\dagger\hat{b}_j] \right\} \rho_m, \quad (\text{S30})
\end{aligned}$$

where \tilde{H} is the effective Hamiltonian that has been renormalized by the interaction with the cavity field. The explicit form of \tilde{H} is given by

$$\begin{aligned}
\tilde{H} &= \sum_{i=1}^N \omega_i \hat{b}_i^\dagger \hat{b}_i + \sum_{i=1}^N U_{i,i}^2 \left[\tilde{\Delta}(2\omega_i)\hat{b}_i^\dagger\hat{b}_i^\dagger\hat{b}_i\hat{b}_i + \tilde{\Delta}(-2\omega_i)\hat{b}_i\hat{b}_i\hat{b}_i^\dagger\hat{b}_i^\dagger + \tilde{\Delta}(0)(\hat{b}_i^\dagger\hat{b}_i + \hat{b}_i\hat{b}_i^\dagger)^2 \right] \\
&\quad + \sum_{i<j} 4U_{i,j}^2 \left[\tilde{\Delta}(\omega_i + \omega_j)\hat{b}_i^\dagger\hat{b}_j^\dagger\hat{b}_j\hat{b}_i + \tilde{\Delta}(-\omega_i - \omega_j)\hat{b}_i\hat{b}_j\hat{b}_j^\dagger\hat{b}_i^\dagger + \tilde{\Delta}(\omega_i - \omega_j)\hat{b}_i^\dagger\hat{b}_j\hat{b}_j^\dagger\hat{b}_i + \tilde{\Delta}(\omega_j - \omega_i)\hat{b}_i\hat{b}_j^\dagger\hat{b}_j\hat{b}_i^\dagger \right] \quad (\text{S31})
\end{aligned}$$

Since \tilde{H} only contains phonon number operators \hat{n}_i , \hat{n}_j and their products, it will not influence the dynamics of average phonon numbers. From the master equation for the reduced density operator ρ_m , we can obtain the rate equations for the average phonon numbers

$$\begin{aligned}
\langle \dot{\hat{n}}_l \rangle &= -\gamma_l(\langle \hat{n}_l \rangle - \bar{n}_{l,\text{th}}) - 2U_{l,l}^2\Gamma(2\omega_l)\langle \hat{n}_l(\hat{n}_l - 1) \rangle + 2U_{l,l}^2\Gamma(-2\omega_l)\langle (\hat{n}_l + 1)(\hat{n}_l + 2) \rangle \\
&\quad + \sum_{j \neq l} -4U_{j,l}^2\Gamma(\omega_l + \omega_j)\langle \hat{n}_l\hat{n}_j \rangle + 4U_{j,l}^2\Gamma(-\omega_l - \omega_j)\langle (\hat{n}_l + 1)(\hat{n}_j + 1) \rangle \\
&\quad + \sum_{j \neq l} -4U_{j,l}^2\Gamma(\omega_l - \omega_j)\langle \hat{n}_l(\hat{n}_j + 1) \rangle + 4U_{j,l}^2\Gamma(\omega_j - \omega_l)\langle (\hat{n}_l + 1)\hat{n}_j \rangle. \quad (\text{S32})
\end{aligned}$$

The physical meaning of Eq. (S32) is explained as follows. In the first line, the first term describes the dissipation (one-phonon process) caused by the heat bath, the second and the third term describe the absorption and emission of two phonons at the l th mode, which are the well-known two-phonon sideband cooling and heating processes. The second line describes another kind of sideband cooling and heating processes, where instead of absorption or emission of two phonons at the same mode, the simultaneous absorption or emission of a phonon at the l th mode and a phonon at the j th mode happened. The third line describes the energy-redistribution processes (two-phonon process), where the first term describes the absorption of a phonon with energy $\hbar\omega_l$ in conjunction with emission of a phonon with energy $\hbar\omega_j$, and the second term describes the reverse processes. To close Eq. (S32), we make the decorrelation approximation $\langle \hat{n}_l \hat{n}_j \rangle \approx \langle \hat{n}_l \rangle \langle \hat{n}_j \rangle$ with the assumption that the fluctuations of phonon numbers are much less than the average phonon numbers. Unlike Fröhlich's results, we are unable to solve the steady states of these equations analytically in this case of large N .

The spectral shape of rate $\Gamma(\omega)$ is Lorentzian that is centered at $-\Delta$ with linewidth κ . We choose $\Delta \approx \pm|\omega_l - \omega_j|$ and assume that the eigenfrequency band is narrow ($|\omega_l - \omega_j| \ll \omega_l, \omega_j$), then $\Gamma(\pm 2\omega_l) \ll \Gamma(\pm|\omega_j - \omega_l|)$. Furthermore, we assume the side-band cooling and heating processes are much weaker than the dissipation, i.e., $U_{l,l}^2 \Gamma(\pm 2\omega_l) \langle \hat{n}_l \rangle \ll \gamma_l$. This approximation is well satisfied by the experimental parameters we used. In this case we can neglect the sideband cooling and heating processes. The rate equations are simplified to

$$\dot{\langle \hat{n}_l \rangle} = -\gamma_l (\langle \hat{n}_l \rangle - \bar{n}_{l,\text{th}}) + \sum_{j \neq l} 4U_{j,l}^2 [\Gamma(\omega_j - \omega_l) \langle (\hat{n}_l + 1) \hat{n}_j \rangle - \Gamma(\omega_l - \omega_j) \langle \hat{n}_l (\hat{n}_j + 1) \rangle]. \quad (\text{S33})$$

when $U_{l,l}^2 \Gamma(\pm 2\omega_l) \langle \hat{n}_l \rangle \sim \gamma_l$, we should use the full rate equations.

To verify the approximations we make above, we compare the numerical results obtained from the full quantum master equation (Eq. (S10)), the reduced quantum master equation (Eq. (S30)), the rate equations (Eq. (S32)) and the rate equations without heating and cooling processes (Eq. (S33)), as shown in Fig. (S1). The quantum master equations are solved by the steady-state solver of QuTiP package [3]. The rate equations are solved by the 5th-order-Runge-Kutta-Cash-Karp method. The states at $t = 200$ s, at which time the states have reached the constant, are chosen as the steady states. From the figure, it is seen that the results of full quantum master equation and reduced master equation are in excellent agreement, which demonstrates the validity of Born-Markov approximation and rotating-wave approximation. The agreement between rate equations with and without heating/cooling processes shows the small contribution of heating/cooling processes. The small deviation between the results of master equation and rate equations at large optomechanical couplings may be due to the cutoff of the dimension of Hilbert space in the calculation of master equations and the decorrelation approximation.

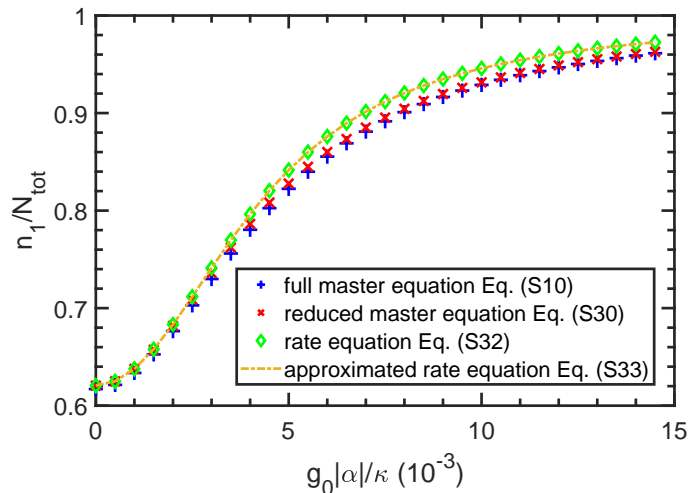


FIG. S1. The steady-state ratio of average phonon number at the lowest mechanical mode with respect to optomechanical couplings. $N = 2$, $T = 1$ mK, $\omega_0 = 100$ MHz, $k/m = \omega_0^2/3$, $\kappa = 1$ MHz, $\gamma_1 = \gamma_2 = 100$ Hz, $\Delta = -k/(m\omega_0)$. The thermal phonon population is $\bar{n}_{1,\text{th}} = 1.15$, $\bar{n}_{2,\text{th}} = 0.71$. The cutoff of Fock state is set to 10 for phonons, and set to 5 for photon in the calculation of the master equations.

Summing Eq. (S33) over l , we obtain

$$\dot{\langle \hat{N}_{\text{tot}} \rangle} = -\sum_l \gamma_l (\langle \hat{n}_l \rangle - \bar{n}_{l,\text{th}}), \quad (\text{S34})$$

where $\langle \hat{N}_{\text{tot}} \rangle = \sum_l \langle \hat{n}_l \rangle$ is the total phonon number. We assume that $\gamma_l = \gamma$, then the evolution of total phonon number only depends on γ and the thermal phonon populations. The steady state of $\langle \hat{N}_{\text{tot}} \rangle$ is given by

$$\langle \hat{N}_{\text{tot}} \rangle = \sum_l \langle \bar{n}_{l,\text{th}} \rangle. \quad (\text{S35})$$

COMPARISON BETWEEN FRÖHLICH ORIGINAL MODEL AND OUR MODEL

The rate equations of Fröhlich original result are

$$\dot{n}_l = s - \phi(n_l e^{\hbar\omega_l/KT} - (n_l + 1)) + \chi \sum_j [(n_l + 1)n_j - n_l(1 + n_j)e^{\hbar(\omega_l - \omega_j)/KT}] \quad (\text{S36})$$

On the right-hand side of Eq. (S36), the first term describes the incoherent phonon pumping, the second term describes the dissipation induced by the heat bath, and the third term describes the two-phonon-energy-redistribution processes. The second term of Eq. (S36) is the same as the dissipation term of Eq. (S33) when we make use of the identity

$$e^{\hbar\omega_l/KT} = \frac{\bar{n}_{l,\text{th}} + 1}{\bar{n}_{l,\text{th}}} \quad (\text{S37})$$

If there is no phonon pumping, i.e. $s = 0$, the steady state of phonon distribution follows the thermal distribution. Thus, the main differences between Fröhlich original model (Eq. (S36)) and our model (Eq. (S33)) are: (i) *the incoherent phonon pumping is optional in our model, while the phonon pumping is necessary in Fröhlich original model*; (ii) *the two-phonon-energy-distribution processes in our model can be controlled by the driving laser, while these processes in Fröhlich original model are determined by the environment*.

TIME EVOLUTION OF PHONON NUMBERS

To observe the coherence of Fröhlich condensate, we want the time needed to achieve Fröhlich condensate to be shorter than the coherence time.

In Fig. (S2a), we show the evolution of average phonon numbers at different optomechanical couplings in the case of $N = 5$. It can be seen the evolution is faster for larger optomechanical couplings. The evolution rate of average phonon numbers mainly depends on the energy-redistribution processes, i.e., the net transition rate $\Gamma_{j \rightarrow 1}$. In Fig. (S2b), we show the time t_c for $\langle \hat{n}_1 \rangle / \langle \hat{N}_{\text{tot}} \rangle$ to reach 90% of its peak value with respect to the optomechanical coupling. The numerical results fit well with the prediction $t_c \propto \Gamma_{j \rightarrow 1} \propto g_0^2 |\bar{\alpha}|^{-2}$. As a simple example, we choose $g_0^2 |\bar{\alpha}| / \kappa = 2 \times 10^{-5}$. In Fig. (S2b), the condensation time is less than 5 second. Using the same parameters, we find the coherence time is greater than 40 second, as shown in Fig. (5) of the main text. Thus, the coherence time is much longer than the time needed to achieve to condensation.

THE DEPENDENCE OF PHONON NUMBERS ON OPTOMECHANICAL COUPLING, TEMPERATURE AND EXTERNAL PHONON PUMPING

In Fig. (S3) and (S4), we show the dependence of steady-state ratio $\langle n_1 \rangle / \langle \hat{N}_{\text{tot}} \rangle$ with respect to the optomechanical coupling and temperature. Since the rate equations cannot be solved analytically, here we gives an order of magnitude estimate of the critical condition.

The starting point is the rate equation for the phonon numbers at the lowest mode,

$$\langle \dot{\hat{n}}_1 \rangle = -\gamma(\langle \hat{n}_1 \rangle - \bar{n}_{1,\text{th}}) + \sum_{j=2}^N 4U_{j,1}^2 [\Gamma(\omega_j - \omega_1)(\langle \hat{n}_1 \rangle + 1)\langle \hat{n}_j \rangle - \Gamma(\omega_1 - \omega_j)\langle \hat{n}_1 \rangle(\langle \hat{n}_j \rangle + 1)]. \quad (\text{S38})$$

If the Fröhlich condensate is achieved, we can assume $\langle \hat{n}_1 \rangle = a \langle \hat{N}_{\text{tot}} \rangle$, where a is a number close to 1. For large N , the total phonon number $\langle \hat{N}_{\text{tot}} \rangle \gg \bar{n}_{1,\text{th}}$, then Eq. (S38) at steady state can be simplified as

$$\gamma a \langle \hat{N}_{\text{tot}} \rangle \approx 4a \langle \hat{N}_{\text{tot}} \rangle \sum_{j=2}^N U_{j,1}^2 [\Gamma(\omega_j - \omega_1) - \Gamma(\omega_1 - \omega_j)] \langle \hat{n}_j \rangle \quad (\text{S39})$$

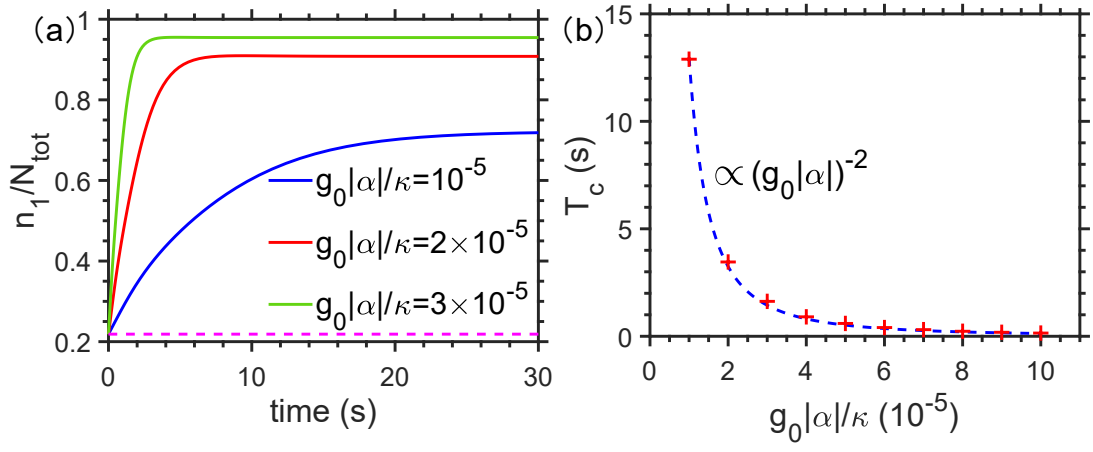


FIG. S2. Time evolution of the ratio of the average phonon numbers at the lowest mode to the total phonon numbers. (a) Time evolution of $\langle \hat{n}_1 \rangle / \langle \hat{N}_{\text{tot}} \rangle$ at different optomechanical couplings. (b) The time needed for $\langle \hat{n}_1 \rangle / \langle \hat{N}_{\text{tot}} \rangle$ to achieve 90% of the peak value with respect to optomechanical couplings. The number of membranes $N = 5$. The membrane and cavity parameters we use are similar to those in Ref. [1, 2]. $\omega_0 = 1$ MHz, $\kappa = 100$ kHz, $\gamma = 0.1$ Hz, $T = 300$ mK, the thermal phonon population \bar{n}_{th} is at the order of 10^4 . The mechanical coupling and detuning are chosen as $k/m = \omega_0^2/10$, $\Delta = -k/(m\omega_0)$. The dashed line in (a) denotes $\bar{n}_{1,\text{th}}/\hat{N}_{\text{tot}}$ in thermal equilibrium.

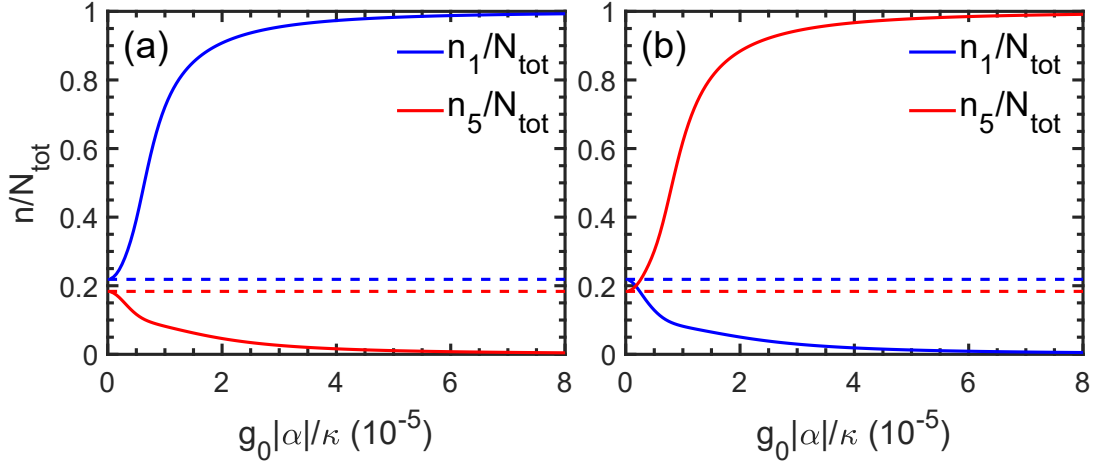


FIG. S3. The steady-state ratio of phonon numbers with respect to optomechanical coupling. $N = 5$. (a) Negative detuning $\Delta = -k/(m\omega_0)$. (b) Positive detuning $\Delta = k/(m\omega_0)$. The other parameters are the same as those used in Fig. (S2). The blue (red) dashed line denotes the ratio of phonon numbers at the lowest (highest) mode in thermal equilibrium.

To estimate the order of magnitude of the summation on the right hand-side of Eq. (S39), we first plot the steady-state average phonon distribution of the Fröhlich condensate with $\langle \hat{n}_1 \rangle / \langle \hat{N}_{\text{tot}} \rangle = 0.99$, and the corresponding net transition rate from the j th mode to the lowest mode $\Gamma_{j \rightarrow 1}$ in the case of $N = 70$, as shown in Fig. (S5). It can be seen that while the rest of phonons mainly occupy the second mode, the net transition rates from different high frequency modes to the lowest mode are at the same order of magnitude. Based on this observation, we assume the phonon number at the second mode is approximately $(1 - a)\langle \hat{N}_{\text{tot}} \rangle$ and consider the transition from the second mode to the lowest mode

$$\Gamma_{2 \rightarrow 1} \approx 4a\langle \hat{N}_{\text{tot}} \rangle U_{2,1}^2 [\Gamma(\omega_2 - \omega_1) - \Gamma(\omega_1 - \omega_2)] (1 - a)\langle \hat{N}_{\text{tot}} \rangle. \quad (\text{S40})$$

In the large N limit, the frequency difference between the first two modes satisfies $\omega_2 - \omega_1 \sim k/(m\omega_0 N^2) \ll |\Delta|, \kappa$. Expanding $\Gamma(\omega_2 - \omega_1) - \Gamma(\omega_1 - \omega_2)$ to the first order of $\omega_2 - \omega_1$ and making use of the formula of $U_{2,1}^2$, we obtain the order of magnitude estimate of the net transition rate $\Gamma_{2 \rightarrow 1}$

$$\Gamma_{2 \rightarrow 1} \sim \frac{6000\pi^6 a(1 - a)k\kappa|\Delta|g_0^2|\bar{\alpha}|^2}{m\omega_0(\kappa^2 + 4\Delta^2)^2 N^8} \langle \hat{N}_{\text{tot}} \rangle^2. \quad (\text{S41})$$

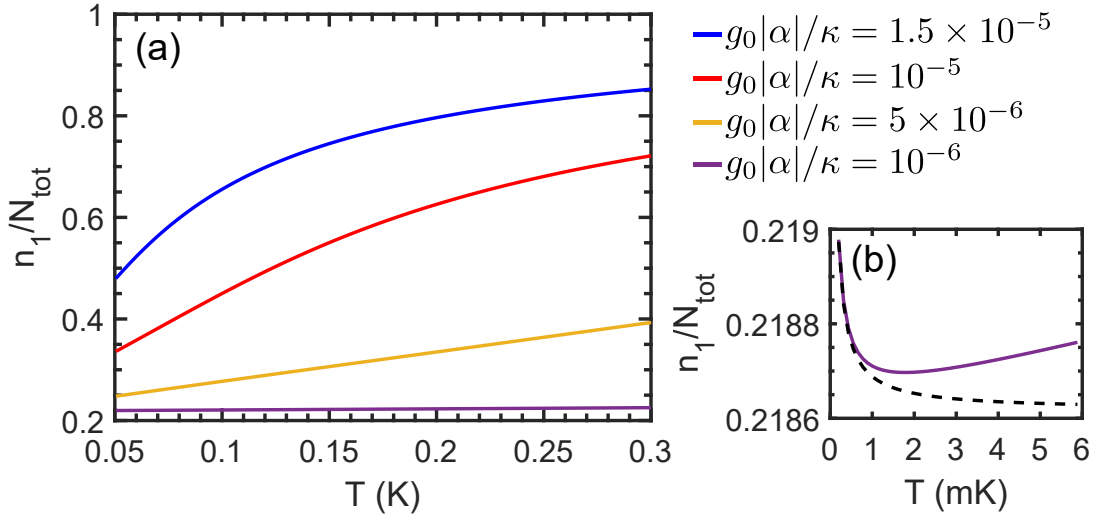


FIG. S4. The steady-state ratio of phonon numbers with respect to temperature. $N = 5$. (a) $\langle n_1 \rangle / \langle \hat{N}_{\text{tot}} \rangle$ with respect to temperature at different optomechanical couplings. (b) $\langle n_1 \rangle / \langle \hat{N}_{\text{tot}} \rangle$ at low temperature regime. The dashed line is the population given by the thermal distribution. The other parameters are the same as those used in Fig. (S2).

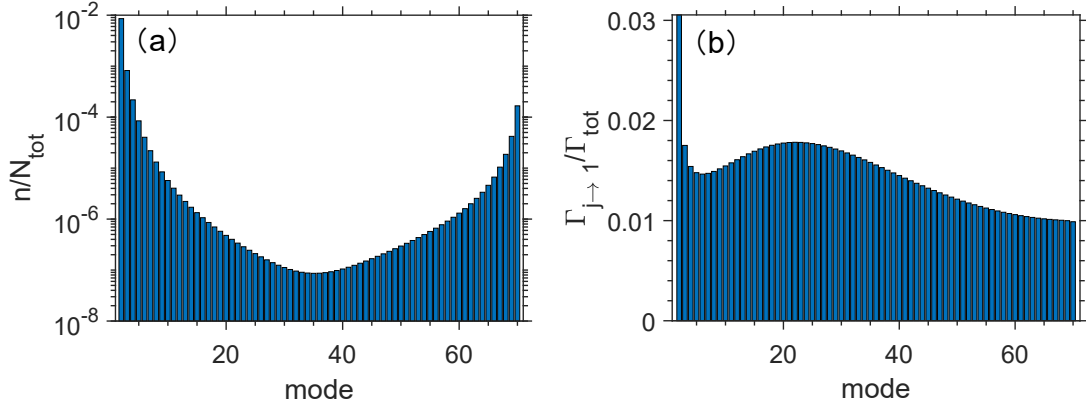


FIG. S5. The steady state of a Fröhlich condensate with $\langle \hat{n}_1 \rangle / \langle \hat{N}_{\text{tot}} \rangle = 0.99$. (a) Phonon distribution in $j \geq 2$ modes. (b) The net transition rate from the j th mode to the lowest mode. $N = 70$, $g_0|\bar{\alpha}| = 0.06\kappa$, the other parameters are the same as those used in Fig. (S2).

The total transition rate from high frequency modes to the lowest one is approximately $N\Gamma_{2 \rightarrow 1}/2$, which should be equal to the dissipation rate $\gamma a \langle \hat{N}_{\text{tot}} \rangle$ at the steady state. Then we can obtain the critical condition required to achieve Fröhlich condensate

$$\frac{3000\pi^6(1-a)k\kappa|\Delta|g_0^2|\bar{\alpha}|^2\bar{n}_{\text{th}}}{m\omega_0\gamma(\kappa^2+4\Delta^2)^2} \sim N^6, \quad (\text{S42})$$

where we have made use of Eq. (S35) and $\bar{n}_{\text{th}} = \frac{1}{N} \sum_l \langle \bar{n}_{l,\text{th}} \rangle$ is the mean thermal phonon number. In the limit of $k_B T \gg \hbar\omega_0$, we have $\bar{n}_{\text{th}} \approx \frac{k_B T}{\hbar\omega_0}$, where k_B is the Boltzmann constant.

The incoherent phonon pumping in Fröhlich's original model can also be introduced to our system. To account for the effect of incoherent phonon pumping, we introduce the pumping rate Γ_p on the right-hand side of Eq. (S33). Then Eq. (S34) is modified as

$$\langle \dot{\hat{N}}_{\text{tot}} \rangle = N\Gamma_p - \sum_l \gamma(\langle \hat{n}_l \rangle - \bar{n}_{l,\text{th}}), \quad (\text{S43})$$

The steady state of $\langle \hat{N}_{\text{tot}} \rangle$ is given by $\langle \hat{N}_{\text{tot}} \rangle = \frac{N\Gamma_p}{\gamma} + \sum_l \langle \bar{n}_{l,\text{th}} \rangle$. Hence, the introduction of incoherent phonon

pumping is equivalent to an effective temperature of the system $T_{\text{eff}} \approx T + \frac{\hbar\omega_0\Gamma_p}{k_B\gamma}$. In Fig. (S6), we show the contour of $\langle \hat{n}_1 \rangle / \langle \hat{N}_{\text{tot}} \rangle$ with respect to optomechanical coupling, temperature and incoherent phonon pumping.

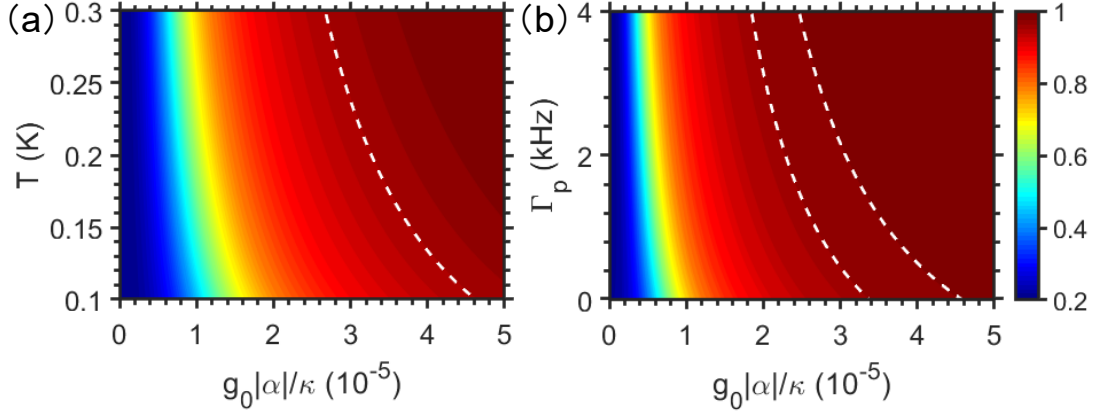


FIG. S6. The contour of $\langle \hat{n}_1 \rangle / \langle \hat{N}_{\text{tot}} \rangle$ in steady state with respect to $g_0|\bar{\alpha}|$, temperature or external phonon pumping. (a) No phonon pumping. The dashed line fitted by Eq. (S42) agrees well with the contour lines $\langle \hat{n}_1 \rangle / \langle \hat{N}_{\text{tot}} \rangle = 0.945$. (b) With phonon pumping. $T = 0.3$ K is fixed. The dashed lines are fitted by Eq. (S42) with \bar{n}_{th} replaced by $\frac{\Gamma_p}{\gamma} + \bar{n}_{\text{th}}$, which agree well the contour line $\langle \hat{n}_1 \rangle / \langle \hat{N}_{\text{tot}} \rangle = 0.966$ and $\langle \hat{n}_1 \rangle / \langle \hat{N}_{\text{tot}} \rangle = 0.98$. $N = 5$, the other parameters are the same as those used in Fig. (S2).

THE COHERENCE OF FRÖHLICH CONDENSATE

To describe the coherence of the lowest mode, we use the first-order correlation function,

$$G^{(1)}(t, t + \tau) \propto \langle \hat{b}_1^\dagger(t) \hat{b}_1(t + \tau) \rangle. \quad (\text{S44})$$

The evolution of the correlation function can be derived via the quantum regression formula. From Eq. (S30), we can calculate the equation of motion for the mean amplitude of the lowest mode:

$$\begin{aligned} \dot{\langle \hat{b}_1 \rangle} = & -i \left\{ \omega_1 \langle \hat{b}_1 \rangle + 2U_{1,1}^2 \left[\tilde{\Delta}(2\omega_1) \langle \hat{n}_1 \hat{b}_1 \rangle + \tilde{\Delta}(-2\omega_1) (\langle \hat{n}_1 \hat{b}_1 \rangle + 2\langle \hat{b}_1 \rangle) + 4\tilde{\Delta}(0) (\langle \hat{n}_1 \hat{b}_1 \rangle + \langle \hat{b}_1 \rangle) \right] \right. \\ & + \sum_{j=2}^N 4U_{j,1}^2 \left[\tilde{\Delta}(\omega_1 + \omega_j) \langle \hat{n}_j \hat{b}_1 \rangle + \tilde{\Delta}(-\omega_1 - \omega_j) (\langle \hat{n}_j \hat{b}_1 \rangle + \langle \hat{b}_1 \rangle) + \tilde{\Delta}(\omega_1 - \omega_j) (\langle \hat{n}_j \hat{b}_1 \rangle + \langle \hat{b}_1 \rangle) + \tilde{\Delta}(\omega_j - \omega_1) \langle \hat{n}_j \hat{b}_1 \rangle \right] \left. \right\} \\ & - \left\{ \frac{\gamma}{2} \langle \hat{b}_1 \rangle + U_{1,1}^2 \left[\Gamma(2\omega_1) \langle \hat{n}_1 \hat{b}_1 \rangle - \Gamma(-2\omega_1) (\langle \hat{n}_1 \hat{b}_1 \rangle + 2\langle \hat{b}_1 \rangle) + 2\Gamma(0) \langle \hat{b}_1 \rangle \right] \right. \\ & + \sum_{j=2}^N 2U_{j,1}^2 \left[\Gamma(\omega_1 + \omega_j) \langle \hat{n}_j \hat{b}_1 \rangle - \Gamma(-\omega_1 - \omega_j) (\langle \hat{n}_j \hat{b}_1 \rangle + \langle \hat{b}_1 \rangle) + \Gamma(\omega_1 - \omega_j) (\langle \hat{n}_j \hat{b}_1 \rangle + \langle \hat{b}_1 \rangle) - \Gamma(\omega_j - \omega_1) \langle \hat{n}_j \hat{b}_1 \rangle \right] \left. \right\}. \quad (\text{S45}) \end{aligned}$$

In the long-time limit, we apply the mean-field approximation, $\langle \hat{n}_1 \hat{b}_1 \rangle \approx \langle \hat{n}_1 \rangle \langle \hat{b}_1 \rangle$. Then Eq. (S45) can be written in the form

$$\dot{\langle \hat{b}_1(t) \rangle} = - \left[i\tilde{\omega}(t) + \frac{\tilde{\gamma}(t)}{2} \right] \langle \hat{b}_1(t) \rangle, \quad (\text{S46})$$

with the formulas of $\tilde{\omega}(t)$ and $\tilde{\gamma}(t)$ given by

$$\begin{aligned}\tilde{\omega}(t) &= \omega_1 + 2U_{1,1}^2 \left[\tilde{\Delta}(2\omega_1)\langle\hat{n}_1\rangle + \tilde{\Delta}(-2\omega_1)(\langle\hat{n}_1\rangle + 2) + 4\tilde{\Delta}(0)(\langle\hat{n}_1\rangle + 1) \right] \\ &\quad + \sum_{j=2}^N 4U_{j,1}^2 \left[\tilde{\Delta}(\omega_1 + \omega_j)\langle\hat{n}_j\rangle + \tilde{\Delta}(-\omega_1 - \omega_j)(\langle\hat{n}_j\rangle + 1) + \tilde{\Delta}(\omega_1 - \omega_j)(\langle\hat{n}_j\rangle + 1) + \tilde{\Delta}(\omega_j - \omega_1)\langle\hat{n}_j\rangle \right] \\ \tilde{\gamma}(t) &= \gamma + 2U_{1,1}^2 \left[\Gamma(2\omega_1)\langle\hat{n}_1\rangle - \Gamma(-2\omega_1)(\langle\hat{n}_1\rangle + 2) + 2\Gamma(0) \right] \\ &\quad + \sum_{j=2}^N 4U_{j,1}^2 \left[\Gamma(\omega_1 + \omega_j)\langle\hat{n}_j\rangle - \Gamma(-\omega_1 - \omega_j)(\langle\hat{n}_j\rangle + 1) + \Gamma(\omega_1 - \omega_j)(\langle\hat{n}_j\rangle + 1) - \Gamma(\omega_j - \omega_1)\langle\hat{n}_j\rangle \right].\end{aligned}\quad (\text{S47})$$

According to the quantum regression formula, the equation of motion for the two-time correlation function is given by

$$\partial_\tau \langle \hat{b}_1^\dagger(t) \hat{b}_1(t + \tau) \rangle = - \left[i\tilde{\omega}(t + \tau) + \frac{\tilde{\gamma}(t + \tau)}{2} \right] \langle \hat{b}_1^\dagger(t) \hat{b}_1(t + \tau) \rangle, \quad (\text{S48})$$

The coherence of the condensate is characterized by the coherence decay rate $\tilde{\gamma}(t)$. At the long-time limit, the average phonon numbers have reached the steady state, then $\tilde{\gamma}(t)$ becomes time independent. Combining Eq. (S32) and Eq. (S47), we can simplify the coherence decay rate as

$$\tilde{\gamma} = \frac{\gamma \bar{n}_{1,\text{th}}}{\langle\hat{n}_1\rangle} + 2U_{1,1}^2 \left[\Gamma(2\omega_1) + \Gamma(-2\omega_1) \left(1 + \frac{2}{\langle\hat{n}_1\rangle} \right) + \Gamma(0) \right] + \sum_{j=2}^N 4U_{j,1}^2 \left[\Gamma(-\omega_1 - \omega_j) \frac{\langle\hat{n}_j\rangle}{\langle\hat{n}_1\rangle} + \Gamma(\omega_j - \omega_1) \frac{\langle\hat{n}_j + 1\rangle}{\langle\hat{n}_1\rangle} \right], \quad (\text{S49})$$

which gives Eq. (7) of the main text. In Fig. S7, we show the evolution of correlation function and its spectral density. An exponential decay and oscillation of the correlation function can be clearly seen. In the simulations, we choose $t = 200$ s, at which time the average phonon numbers have reached the steady state. The upper limit of τ we use is 5000 s.

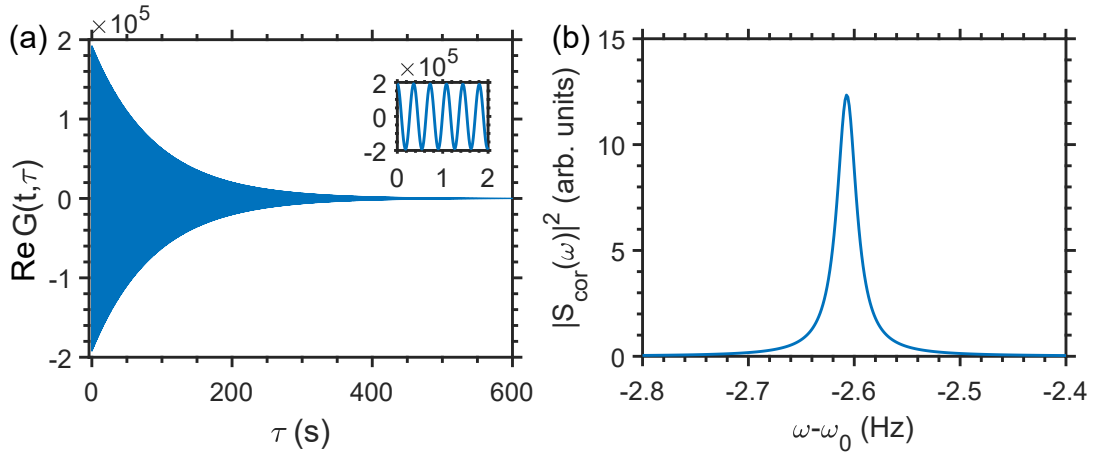


FIG. S7. Time evolution of correlation function and spectra. (a) The time evolution of the real part of the two-time correlation function. The inset shows the enlargement of the first 2 second. Here we have transferred to a frame rotating at ω_1 . (b) The spectral density of correlation function. $N = 5$ and $g_0|\bar{\alpha}|/\kappa = 5 \times 10^{-5}$. t is chosen as 200 second so that average phonon number has reached the steady state. The other parameters are the same as those used in Fig. (S2).

EXPERIMENTAL FEASIBILITY

Here we estimate the experimental feasibility by using existing available systems. The parameters we used are shown in Table. (I).

N	Membrane size	$\omega_0/2\pi$	Mass	Q_m	λ	κ	$G/2\pi$	k/m	Δ	T	P_{in}
5	1 mm \times 1 mm \times 50 nm	134 kHz	40 ng	1.2×10^7	1064 nm	300 kHz	15 MHz \cdot nm $^{-2}$	$\frac{\omega_0^2}{10}$	$\frac{-k}{m\omega_0}$	300 mK	5 μ W
5	100 μ m \times 100 μ m \times 50 nm	1.34 MHz	400 pg	1.2×10^6	1064 nm	300 kHz	15 MHz \cdot nm $^{-2}$	$\frac{\omega_0^2}{10}$	$\frac{-k}{m\omega_0}$	300 mK	7 mW

TABLE I. Membrane and cavity parameters and the estimated power of driving laser.

In the second row of Table. (I), we use the membrane and cavity parameters of Ref. [2]. The required power of driving laser has already discussed in the main text.

The optomechanical system is scalable. In the third row of Table. (I), we decrease the size of membrane to 100 μ m \times 100 μ m \times 50 nm, the resonance frequency increases to $\omega_0 = 2\pi \times 1.34$ MHz, the mass decreases to $m = 400$ pg. Usually, the Q factor will decrease as the size decreases [4, 5]. We assume the Q factor of membranes decreases to $Q_m = 1.2 \times 10^6$ (namely changes 10 times) and the corresponding decay rate becomes $\gamma = 7$ Hz. We further assume the coupling G and the optical decay rate κ do not change, the coupling between membranes and the detuning still follow $k/m = \omega_0^2/10$ and $\Delta = -k/(m\omega_0)$. In this case, the required laser power is $P_{\text{in}} \approx 7$ mW. This power is achievable in optomechanical experiments [6]. Of course, one can also assume the Q value does not change [2], then the laser power required should be $P_{\text{in}} \approx 700 \mu$ W, which is also available in the lab.

We can also estimate the vibrational amplitude of the membranes when the Fröhlich condensate is achieved. The parameters of 1 mm \times 1 mm \times 50 nm Si₃N₄ membrane are used. The temperature is $T = 300$ mK. At the state of Fröhlich condensate, the phonons mainly occupy the lowest mode, the phonon number of the lowest mode is approximately $\frac{Nk_B T}{\hbar\omega_0}$, then the total energy concentrated at the lowest mode is $\frac{Nk_B T}{\hbar\omega_0} \hbar\omega_1 \approx Nk_B T$. The amplitude of the membranes can be estimated by the relationship $m\omega_1^2 \langle x^2 \rangle = Nk_B T$, which gives the vibrational amplitude $A \approx 0.8$ pm for $N = 5$. This amplitude is detectable in nowadays experiments [1, 7]. The amplitude can be further increased by applying external phonon pumping or increasing the temperature. We can also find the effective temperature of the lowest mode is approximately $NT = 1.5$ K.

-
- [1] J. Thompson, B. Zwickl, A. Jayich, F. Marquardt, S. Girvin, and J. Harris, Strong dispersive coupling of a high-finesse cavity to a micromechanical membrane, *Nature* **452**, 72 (2008).
- [2] J. C. Sankey, C. Yang, B. M. Zwickl, A. M. Jayich, and J. G. Harris, Strong and tunable nonlinear optomechanical coupling in a low-loss system, *Nature Physics* **6**, 707 (2010).
- [3] J. R. Johansson, P. D. Nation, and F. Nori, Qutip: An open-source python framework for the dynamics of open quantum systems, *Computer Physics Communications* **183**, 1760 (2012).
- [4] S. S. Verbridge, J. M. Parpia, R. B. Reichenbach, L. M. Bellan, and H. G. Craighead, High quality factor resonance at room temperature with nanostrings under high tensile stress, *Journal of Applied Physics* **99**, 124304 (2006).
- [5] R. A. Barton, B. Ilic, A. M. Van Der Zande, W. S. Whitney, P. L. McEuen, J. M. Parpia, and H. G. Craighead, High, size-dependent quality factor in an array of graphene mechanical resonators, *Nano Letters* **11**, 1232 (2011).
- [6] M. F. Colombano, G. Arregui, N. E. Capuj, A. Pitanti, J. Maire, A. Griol, B. Garrido, A. Martínez, C. M. Sotomayor-Torres, and D. Navarro-Urrios, Synchronization of optomechanical nanobeams by mechanical interaction, *Physical Review Letters* **123**, 017402 (2019).
- [7] V. Singh, S. Bosman, B. Schneider, Y. M. Blanter, A. Castellanos-Gomez, and G. Steele, Optomechanical coupling between a multilayer graphene mechanical resonator and a superconducting microwave cavity, *Nature Nanotechnology* **9**, 820 (2014).